

Ribosylated BSA Monomer is Severely Toxic to SH-SY5Y Cells*

WEI Yan^{1)**}, WANG Yu-Jing^{1,2)**}, WU Bei-Bei^{1,2)}, ZHANG Ying-Hao¹⁾, HE Rong-Qiao^{1)***}

¹⁾ State Key Laboratory of Brain and Cognitive Sciences, Institute of Biophysics, Chinese Academy of Sciences, Beijing 100101, China;

²⁾ University of Chinese Academy of Sciences, Beijing 100049, China)

Abstract Oligomers, rather than polymers and fibrils, of protein aggregates are thought to be cytotoxic, which is a milestone in the study of protein misfolding and aggregation. Abnormally high level of uric ribose in type 2 diabetic patients and ribosylated animal models indicate that diabetes is not only correlated with metabolic dysfunction in glucose but also ribose. Here, using ribosylation of bovine serum albumin (BSA), we show that ribosylated BSA aggregates and proceeds from a monomer and onto an oligomer and polymer, observed with fluorescence spectrophotometer, atomic force microscopy, transmission electron microscopy and size exclusion chromatography. Ribosylated monomer showed severely cytotoxic to SH-SY5Y cells (a human neuroblastoma cell line) under the observations by assays of CCK-8, LDH activity, TUNEL staining, caspase-3 activity and flow-cytometry, whereas ribosylated oligomer and polymer did not. The cytotoxic effect of the ribosylated monomer likely occurs by inducing neuronal apoptosis through activation of the receptor of AGEs (RAGE) associated with mitogen-activated protein kinases (MAPK) pathways.

Key words ribose, glycation, ribosylation, monomer, polymer, cytotoxicity

DOI: 10.16476/j.pibb.2016.0054

Glycation, which occurs between a reducing sugar and the amino group of protein, results in reversible Schiff's base, stable Amadori products, and finally the irreversibly advanced glycation end products (AGEs). AGEs are well known for their destructive activities in diabetes, where they contribute to vascular disease, kidney failure, eye damage, and other kinds of dysfunction^[1-2] including the nerve damage known as diabetic peripheral neuropathy^[3-5]. In patients with this kind of neuropathy, AGEs directly damage vital components of nerve cells, such as cytoskeleton^[6]. High levels of the reducing sugars accelerate the glycation of protein and produce AGEs in the human body, leading to protein aggregations which are harmful to cells and are involved in the complication of diabetes mellitus^[7]. In addition to diabetes, glycation is also a significant contributory factor in neurodegenerative diseases^[1-4, 8-9]. Thus, investigation of how glycated protein triggers cell death is helpful for understanding the mechanisms of the complications in type 2 diabetes mellitus (T2DM)

progression.

Recently, abnormally high levels of ribose have been found in T2DM^[10], suggesting that T2DM is not only a disorder in glucose metabolism, but also in ribose^[11]. Furthermore, ribose is the most active in glycation of proteins such as bovine serum albumin (BSA)^[12], Tau protein^[13-14] and alpha-synuclein^[15], compared with glucose, fructose and the other reducing sugars. Kong and colleagues also showed that ribosylation is faster than glucosylation^[16]. Ribose glycates proteins and induces aggregation in relatively short time (less than 7 days), activating inflammation

*This work was supported by grants from National Basic Research Program of China (2012CB911004), The National Natural Scientific Foundation of China (31270868, 31200601) and The External Cooperation Program of BIC, Chinese Academy of Sciences (GJHZ201302).

**These authors contributed equally to this work.

***Corresponding author.

Tel: 86-10-64889876, E-mail: herq@sun5.ibp.ac.cn

Received: February 23, 2016 Accepted: May 11, 2016

of brain tissues, leading to neuronal death and cognitive impairment of mice following ribose injection^[17]. Clarifying that the role ribose plays in cell dysfunction will contribute to our understanding of the mechanisms underlying diabetic complications and other aging diseases including age-related cognitive impairment^[18].

Protein aggregates are cytotoxic in their pre-fibrillar organization^[19]. For example, oligomers of amyloid β are commonly thought to be the most cytotoxic to neural cells^[20]. Similar phenomena have also been reported with human islet amyloid polypeptide (h-IAPP)^[21]. The toxic form of amyloidogenic protein oligomers is distinct and smaller than amyloid fibrils and acts by disrupting cellular membranes of β cells^[22]. As we described previously, ribosylation leads to protein glycation, which forms monomer, oligomer or polymer^[12]. Determining which glycated product is most cytotoxic can clarify the mechanisms not only for ribose-induced apoptosis but also for diabetic complications and neurodegenerative diseases.

In the present work, we investigated the effect of long-term ribosylation on neural cells using a previously established ribosylation system. Ribosylated BSA(RBSA) increased in its size in a time dependent manner. Interestingly the glycated monomer, not the polymer and oligomer, showed the highest cytotoxicity through reaction of receptor of AGEs (RAGE) followed by activation of mitogen-activated protein kinases (MAPK) pathways.

1 Materials and methods

1.1 Preparation of ribosylated BSA

BSA (Sigma-Aldrich, USA) was dissolved in 20 mmol/L Tris-HCl (pH 8.0) to yield a stock solution of 20 g/L. This solution was then mixed with D-ribose (Amresco, USA) prepared in Tris-HCl (pH 8.0) buffer to a final concentration of 10 g/L BSA and 1 mol/L D-ribose. BSA alone was used as a control. Reaction mixtures were incubated at 37 °C for 0 day, 3 days, 7 days, 2 weeks, and 8 weeks. All solutions were filtered with 0.22 μ m membranes (Millipore, USA). After incubation, preparations were extensively dialyzed against Tris-HCl buffer to remove free D-ribose.

1.2 Fluorescence measurements

Fluorescence of the advanced glycation end products (AGEs) was monitored on a FluoroMax-4 Spectrofluorometer (HORIBA, Japan). Wavelengths

(λ_{ex} 370 nm/ λ_{em} 425 nm) were employed^[23]. Desired final protein concentration was 0.1 g/L.

1.3 Atomic force microscopy(AFM) measurements

Protein samples were diluted using Tris-HCl buffer (pH 8.0) and 10 μ l of protein (10 μ g) was dropped onto the mica surface and left for 5 min at room temperature before drying with nitrogen gas. The mica diaphragm was rinsed 20 times with ultra-purified water and dried with nitrogen gas before observation under the atomic force microscopy (Mutiplemode - I, Digital Instruments, USA). The horizontal diameter at half height of a particle (globular protein) was measured and data were analyzed using Nanoscope6.11r1 software (USA).

1.4 Transmission electron microscopy (TEM) measurements

Protein samples were diluted using Tris-HCl buffer (pH 8.0) to the final concentration of 1 g/L protein and applied onto glow-discharged, carbon-coated copper grids. The sample was left for 1~2 min on the grids before blotting and staining with a solution of 2% uranyl acetate for 30 s before observation under the transmission electron microscope (Tecnai Spirit, Holland). The particle diameters were measured using Image-Pro Plus 6.0 software.

1.5 Cell culture

Human neuroblastoma cell line SH-SY5Y cells were cultured in Dulbecco's modified Eagle's medium (DMEM, Gibco, USA) supplemented with 100 U/ml penicillin and 100 mg/L streptomycin at 37 °C in a humidified 5% CO₂ incubator as described^[24]. The medium contained 10% fetal bovine serum. Cells were grown to 80%~90% confluence in 100 mm diameter dishes and fed every two day. For all experiments, the culture medium was replaced with serum-free medium before the addition of ribosylated BSA.

1.6 Cell viability test

1.6.1 MTT assay

SH-SY5Y cells were seeded on a 96-well plate at a concentration of 10⁴ cells per well. After 24 h, the culture medium was replaced with serum-free medium in the presence of ribosylated BSA or BSA (15 μ mol/L). Medium without glycated protein was used as a control. After 8 h, 24 h or 48 h of treatment, MTT(final concentration 0.5 g/L) was added and the plates were incubated at 37 °C for 4 h. The assay was stopped by replacement of the MTT-containing medium with 150 μ l dimethylsulfoxide (Amresco,

USA) and the absorbance at 540 nm was measured on a Multiscan MK3 spectrophotometer (Thermo, USA)^[25].

1.6.2 CCK-8 assay

SH-SY5Y cells were seeded on a 96-well plate at a concentration of 10^4 cells per well and exposed to the different ribosylated protein (15 $\mu\text{mol/L}$) after 24 h, except for the control. The cell counting kit-8 (CCK-8, Beyotime, China) reagent was added 24 h later. Plates were incubated at 37 °C for 1 h and the absorbance at 450 nm was recorded on a SpectraMax Paradigm Multi-Mode Detection Platform (Molecular Devices, USA)^[26].

1.7 LDH cytotoxicity detection

LDH cytotoxicity assay was performed with an LDH cytotoxicity assay kit according to the manufacturer's protocol (Beyotime, China)^[27]. Conditions for the cells treatment were the same as described in CCK-8 assay. This colorimetric assay quantifies activity of LDH released from the cytosol of damaged cells into the supernatant and thus serves to quantify cell death.

1.8 Caspase 3 activity assay

In order to detect the caspase 3 activity in SH-SY5Y cells after treatment, caspase 3 activity assay kit was used according to the manufacturer's protocol (Beyotime, China)^[28]. Each measurement was carried out in triplicate.

1.9 Flow cytometric analysis

Cells undergoing apoptosis were detected by double staining with Annexin V-FITC/PI in the dark according to the manufacturer's protocol (Beyotime, China)^[29]. Cells attached to 6-well plate were harvested with 0.25% trypsin and washed twice with PBS. Cells were resuspended in binding buffer. Then the cells were incubated with Annexin V-FITC and propidium iodide (PI) for 10 min at room temperature in the dark. The stained cells were immediately analyzed by flow cytometry (BD FACS Calibur, USA). Each measurement was carried out in triplicate.

1.10 TUNEL-stained assay

DNA damage and cell apoptosis were detected by using the TUNEL assay kit according to the manufacturer's protocol (KeyGEN Biotech, China). Photographs were taken using light microscope (Leica, Germany).

1.11 Gel electrophoresis and Western blotting

Protein samples of ribosylated BSA and cell lysate were mixed with 5 \times SDS-PAGE Sample Buffer (Genstar, China) and boiled for 10 min. Expression

levels of MAP kinases in cells were determined using SDS-PAGE coupled with Western blotting. Cell lysate extracts containing 20~30 μg protein were separated on a 12% SDS-PAGE and then transferred onto PVDF membranes (Millipore). Non-specific binding sites of the membranes were blocked with 5% nonfat milk in PBS containing 0.1% Tween-20 (PBST, pH 7.4) for 1 h at room temperature. The membranes were then incubated overnight at 4 °C with antibodies directed against phospho-Erk, total Erk, phospho-p38, total p38, phospho-JNK, total JNK, or β -actin. The following day, membranes were washed three times with PBST and then incubated for 1 h at room temperature with a horseradish peroxidase-linked secondary anti-mouse or anti-rabbit antibody (Jackson, USA). The membranes were washed again three times, and the immunoreactive bands were then visualized using enhanced chemiluminescence detection reagents (Applygen, Beijing, China). The immunoreactive bands were visualized after exposure of the membranes to Kodak X-ray film and quantified by Quantity One 1D analysis software 4.5.2 (Bio-Rad, Hercules, California, USA).

1.12 Size exclusion chromatography

Size exclusion chromatography was used in order to obtain the different molecular mass fractions of the ribosylated proteins in different incubation time. It was performed on the AKTA PurifierTM 10 (GE Healthcare, Bio-science, USA), using a Superdex 200 column (GE Healthcare, Germany) with a flow rate of 0.5 ml/min in 50 mmol/L phosphate buffer (pH 8.0).

1.13 Data analysis

All values reported are mean \pm SEM. Data analysis was performed by one-way analysis of variance (ANOVA) using Origin 8.0 statistical software. Differences with a probability level of 95% ($P < 0.05$) were considered significant.

2 Results

2.1 Ribosylated BSA acquired cytotoxicity in a time dependent manner

While ribose induces globule-like aggregations of BSA, which becomes cytotoxic in a relatively short time compared with glucose^[12], how ribosylated protein acquires the cytotoxicity is still unknown. Here, we cultured BSA with ribose for different durations (0d, 3d, 7d, 2w and 8w)^[12] and then investigated the modified protein cytotoxicity on human neuroblastoma cell line SH-SY5Y cells using MTT assay at different

time intervals (Figure 1a). No significant changes in the viability of cells, which were incubated with 3-day-ribosylated BSA for 24 h ($P > 0.05$, $n = 3$), was

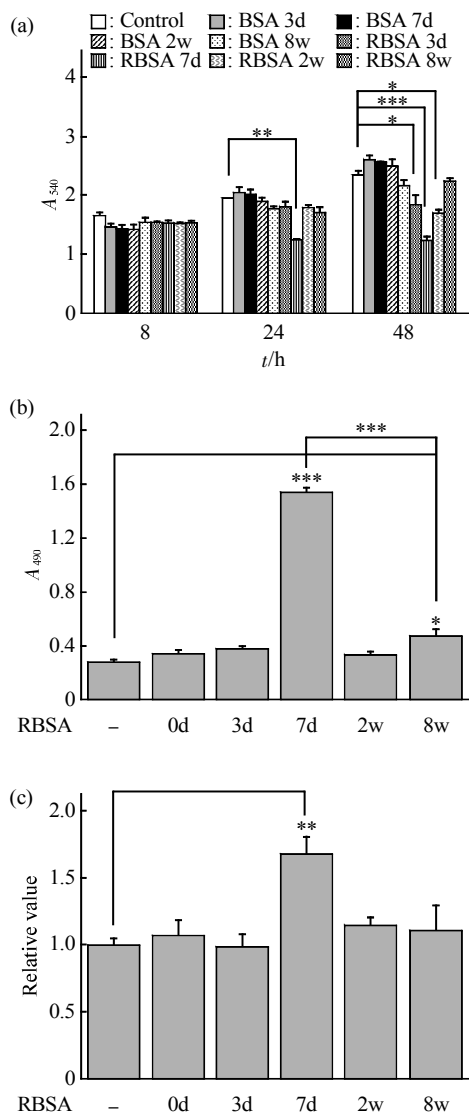


Fig. 1 BSA acquired cytotoxicity depending upon ribosylated time

(a) BSA (final concentration 10 g/L) in the presence of ribose (final concentration 1 mol/L) was kept at 37°C in Tris-HCl buffer (pH 8.0) for different time intervals as indicated (0 d, 3 d, 7 d, 2 w and 8 w). After incubation, aliquots of ribosylated BSA were purified by extensively dialysis against Tris-HCl buffer. Ribosylated BSA at different time intervals were added to SH-SY5Y cells, respectively. Cell viability was measured using the MTT assay at 8 h, 24 h and 48 h after samples addition. All values are expressed as mean ± SEM. * $P < 0.05$, ** $P < 0.01$, *** $P < 0.001$. (b) Conditions for ribosylation were as for Figure 1a except that cells were treated with ribosylated BSA for 24 h. Activities of lactate dehydrogenase (LDH) released from SH-SY5Y cells were assayed. All values are expressed as mean ± SEM. * $P < 0.05$, *** $P < 0.001$. (c) Caspase 3 activity assay was also used to measure the cytotoxicity of ribosylated products after incubation 24 h. The control value in caspase 3 assay was set as 1.0. All values are expressed as mean ± SEM. ** $P < 0.01$.

observed. However following incubation with 7-day-ribosylated BSA for 24 h, viability of SH-SY5Y cells was markedly decreased ($P < 0.01$, $n = 3$), compared with the control. Neither 2-week- nor 8-week-ribosylated BSA had significant effects on the growth of SH-SY5Y cells. To test the viability of cells cultured for 48 h, 7-day-ribosylated BSA still showed the most toxic to cells ($P < 0.001$, $n = 3$) although suppression of the cell viability could be distinctly observed in the presence of 3-day- and 2-week-ribosylated protein ($P < 0.05$).

To determine if cells were damaged in the presence of ribose-glycated BSA, the release of lactate dehydrogenase (LDH) from cells were measured. As exhibited in Figure 1b, 7-day-ribosylated BSA induces the highest cytotoxicity ($P < 0.001$, $n = 3$) showing the most released LDH compared to control after incubation for 24 h. Under the same conditions, the caspase 3 activity is significantly increased ($P < 0.01$, $n = 3$) in the cells incubated with 7-day-ribosylated BSA (Figure 1c), demonstrating the highest cytotoxicity of 7-day-ribosylated BSA and that the caspase 3 pathway is involved in the ribosylation-induced apoptosis.

Flow cytometric analysis, using Annexin V-FITC/PI staining, showed that 7-day-ribosylated BSA was most cytotoxic among all the glycated samples (Figure 2). Seven-day-ribosylated BSA treated cells showed a clear increase in early apoptosis (lower right, LR) in SH-SY5Y cell population after 24 h. Also, the necrotic cell and late apoptosis (upper right, UR) in 7-day-ribosylated BSA treated group was much higher than control and others. Combined above results, we concluded that the acquirement of cytotoxicity for ribosylated BSA depends upon the duration of glycation.

In order to determine if cells proceed in apoptosis in the presence of ribosylated protein, DNA damage inside the cell nucleus was observed. We used a TUNEL assay to stain DNA in SH-SY5Y cells treated with ribosylated BSA for different durations (Figure 3). DNA staining was the most intense after 7-day-ribosylated BSA treatment (Figure 3d) compared to control and other glycated samples (Figures 3a~3c, 3e and 3f). DNase I treated cells were used as a positive control, confirming nuclear intense staining (Figure 3g) and cells incubated without TdT enzyme treatment (Figure 3h) were used as a negative control, which showed no distinct TUNEL staining.

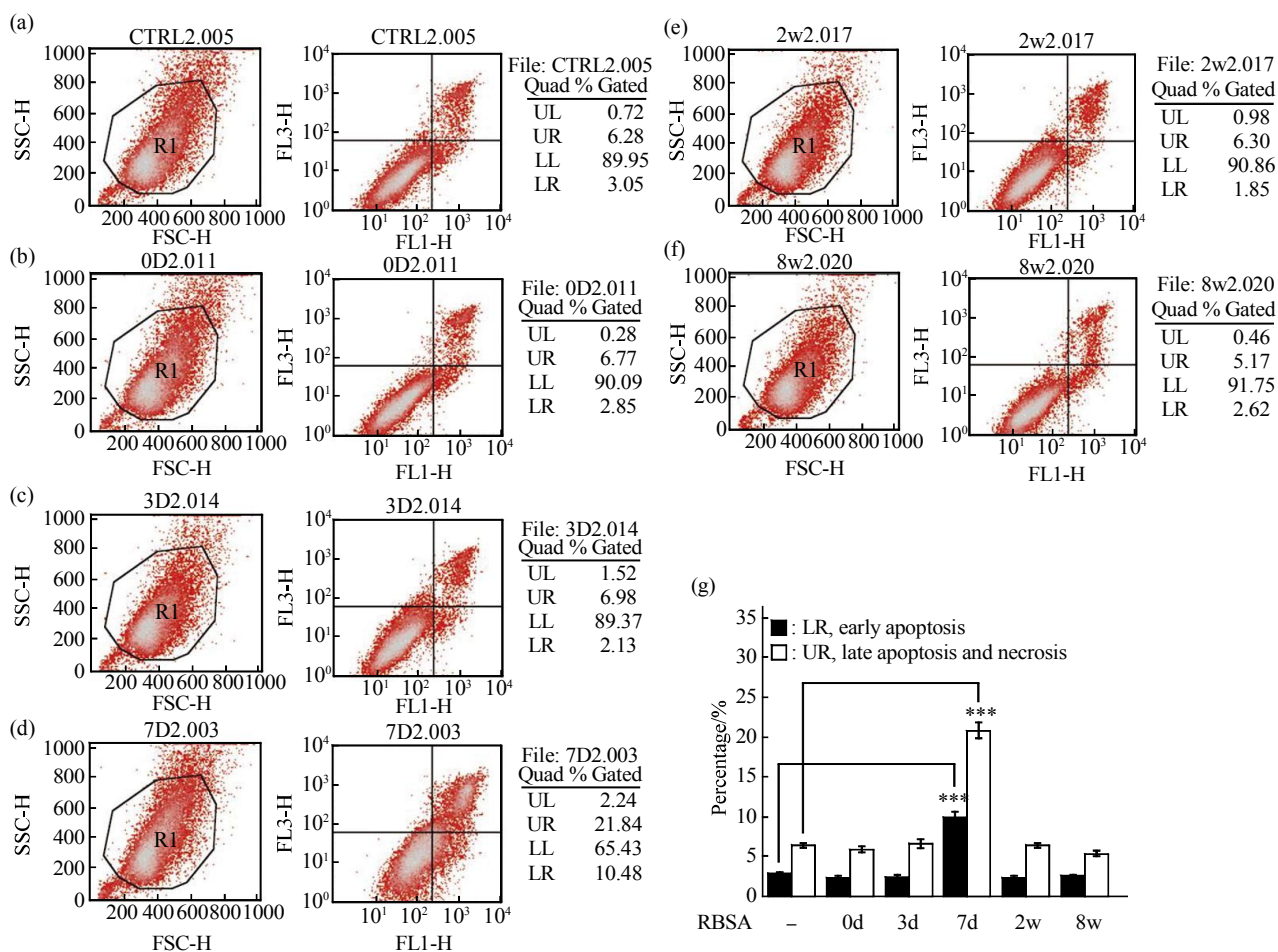


Fig. 2 Apoptosis detection of SH-SY5Y cells cultured with ribosylated BSA

(a) SH-SY5Y cells incubated without ribosylated BSA were used as control. (b~f) Ribosylated BSA at different time intervals (0d, 3d, 7d, 2w and 8w) were added to cells for 24 h and apoptosis was detected by flow cytometric using Annexin V-FITC/PI staining. (g) The statistic results were shown here. All values are expressed as mean \pm SEM. *** $P < 0.001$.

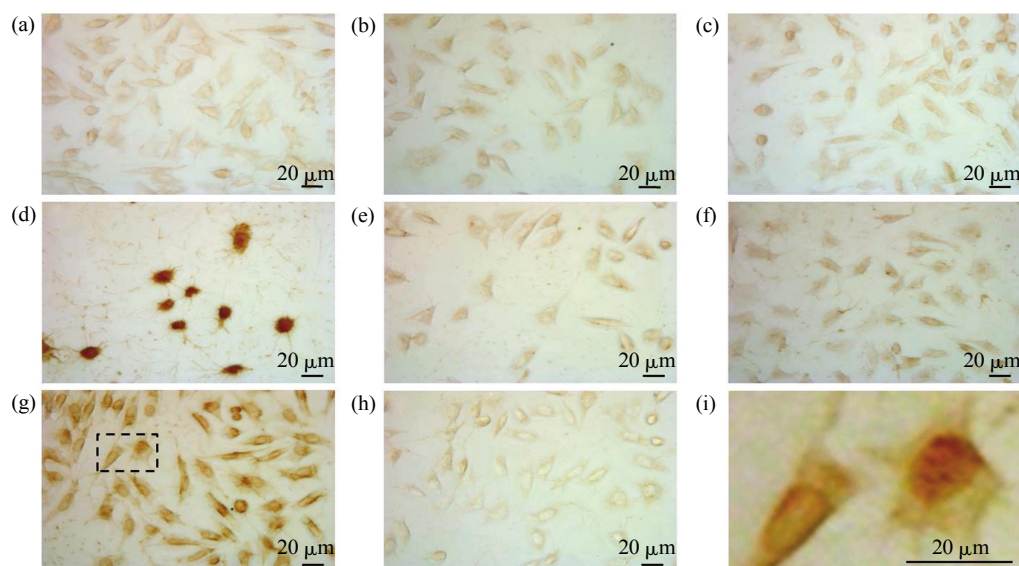


Fig. 3 Microscopic images of SH-SY5Y cells by TUNEL-staining assay

SH-SY5Y cells were treated with ribosylated BSA as described in Figure 1b for 24 h and stained using TUNEL assay. (a) Cells incubated without ribosylated BSA were used as control. (b~f) Cells were incubated with different ribosylated BSA (0d, 3d, 7d, 2w and 8w). Besides, cells treated with DNase I (g) and cells without TdT enzyme treatment (h) were used as positive and negative control, respectively. (i) Magnified image of positive control was also shown here.

2.2 Seven-day-ribosylated BSA mainly existing in monomer

According to Sakono and Zako, cytotoxicity of the amyloid protein depends upon the formation of oligomers but not mature fibrils^[30]. First, we observed changes in the fluorescence at 425 nm by excitation at 370 nm, which is commonly used to detect glycation of a protein^[12, 31]. As shown in Figure 4a, fluorescence increased with the incubation time, indicating that ribosylation occurred between ribose and BSA.

As described by Erickson, the average size (diameter) of BSA is around 7.10 nm measured with

gel-filtration^[32], thus we adopted atomic force microscopy (AFM) and to directly observe the morphological changes in ribosylated BSA. BSA incubated in the absence of ribose was used as control. As shown in Figure 4c, ribose triggered the formation of globular aggregates of BSA, in particular of those incubated over 7 days. Where the size of the protein aggregates increases as the culture time proceeded (insert the statistics) (Figure 4b). The average horizontal diameter at half height of 7-day-ribosylated BSA particles was (6.82 ± 0.21) nm, suggesting a monomer size of the ribosylated protein.

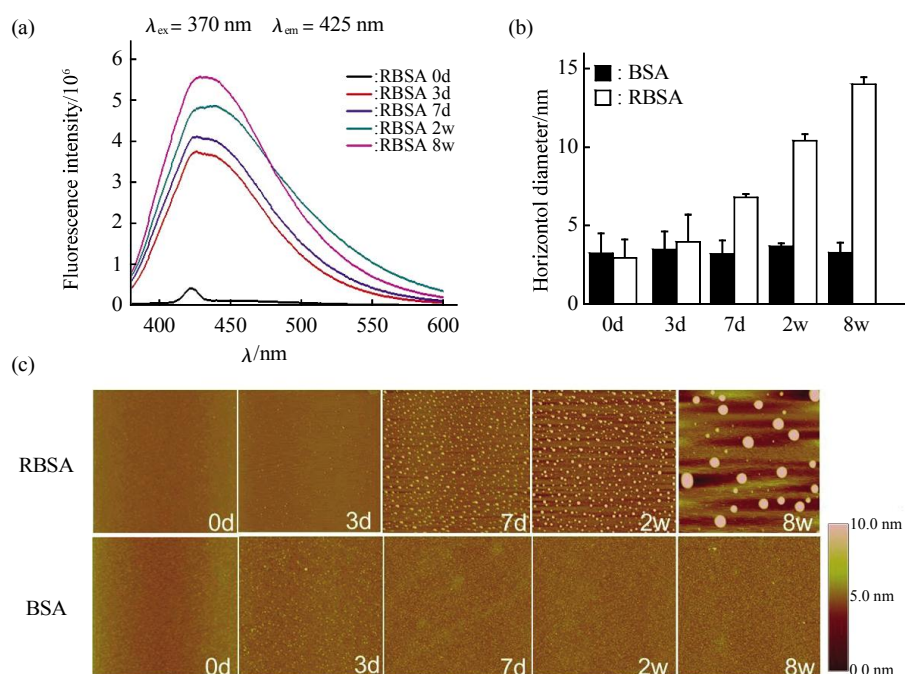


Fig. 4 Fluorescence changes and morphological changes in ribosylation of BSA

(a) Preparation of ribosylated BSA was described in Figure 1a. In order to detect AGEs formation in long-term ribosylation of BSA, the glycation products of BSA were measured with fluorescence ($\lambda_{ex} = 370$ nm, $\lambda_{em} = 425$ nm). (b, c) Ribosylated BSA samples were taken from the incubation mixtures at different time intervals for imaging observation by atomic force microscopy (AFM). BSA alone was used as control. The horizontal diameters (nm) of half height were shown in (b). All values are expressed as mean \pm SEM.

Transmission electron microscopy (TEM) was also used to directly observe the glycosylated protein assembly. Similar results with AFM were shown (Figure 5) that the size of ribosylated BSA increases with time and the average diameter of the particles ribosylated for 7 days is (7.13 ± 0.12) nm, also

suggesting a monomer size of BSA molecule. These data confirmed that most ribosylated BSA particles were in monomers other than in oligomers, polymers and high molecular mass polymers during the incubation for 7 days.

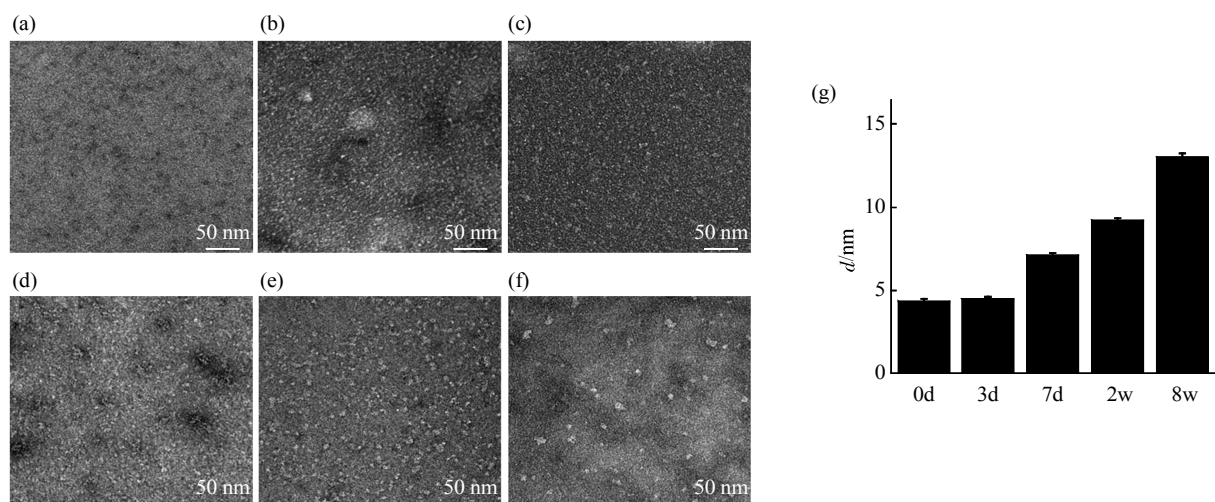


Fig. 5 Morphological changes in ribosylation of BSA by transmission electron microscopy

(a) Tris-HCl buffer solvent was used as negative control. (b~f) Ribosylated BSA samples were taken from the incubation mixtures at different time intervals (0d, 3d, 7d, 2w and 8w) for observation under transmission electron microscopy (TEM). (g) The diameters (d) of protein aggregates were shown here. All values are expressed as mean \pm SEM.

2.3 Ribosylated BSA monomer with a high cytotoxicity

As mentioned above, monomeric 7-day-ribosylated BSA displayed the highest toxicity compared to oligomer and polymer under our experimental conditions. Eight-week-ribosylated BSA showed a little cytotoxicity although it produced the maximal amount of AGEs. Thus, the cytotoxicity may be attributed to the specific size of ribosylated BSA. Seven-day-ribosylated BSA was mostly in monomeric form, while 8-week-ribosylated BSA existed predominately as a polymer and even high molecular mass polymers. Therefore, we used size exclusion chromatography to separate and calculate the diameter of ribose-glycated BSA protein to further investigate whether ribosylated monomer or oligomer or polymer is cytotoxic. Ribosylated BSA for 7 days or less than 7 days mainly showed one peak, while 2-week- and 8-week-glycated protein showed three peaks (Figure 6a). The average diameters of these three peaks were ~ 36.67 nm (polymers), ~ 11.77 nm (oligomers) and ~ 7.52 nm (monomers), respectively (Table 1 and Figure 6b). Sequentially, we collected the protein of three peaks of 8-week-ribosylated BSA, then used the samples to treat SH-SY5Y cells and measured cell

viability with CCK assay. As shown in Figure 6c, only protein of peak 3 (monomers) exhibited significant cytotoxicity ($P < 0.01$, $n = 3$). Ribosylated protein in peak 1 and 2 did not show the toxicity compared to control ($P > 0.05$, $n = 3$). These results demonstrate that ribosylated BSA monomer, but neither oligomers nor polymers, has got highly cytotoxicity.

2.4 Ribosylated BSA leading to cell death through MAPK pathway

Having demonstrated that the ribosylated monomer is cytotoxicity, it is necessary to clarify which pathway is involved in the cell death caused by the glycated monomer. AGEs induces cell apoptosis through activation of MAP kinases^[33], we therefore investigated changes of MAP kinases in SH-SY5Y cells treated with ribosylated BSA monomer. As shown in Figure 7a, phosphorylated MAP kinases p-Erk ($P = 0.0350$, $n = 4$, Figure 7b) and p-p38 ($P = 0.0012$, $n = 4$, Figure 7c) were significantly increased under the treatment of 7-day-ribosylated BSA, indicating the activation of MAPK pathway. No significant changes were observed in p-JNK ($P > 0.05$, $n = 4$, Figure 7d). 3-day-, 2-week-, and 8-week-ribosylated BSA did not significantly affect the levels of the kinases ($P > 0.05$, $n = 4$).

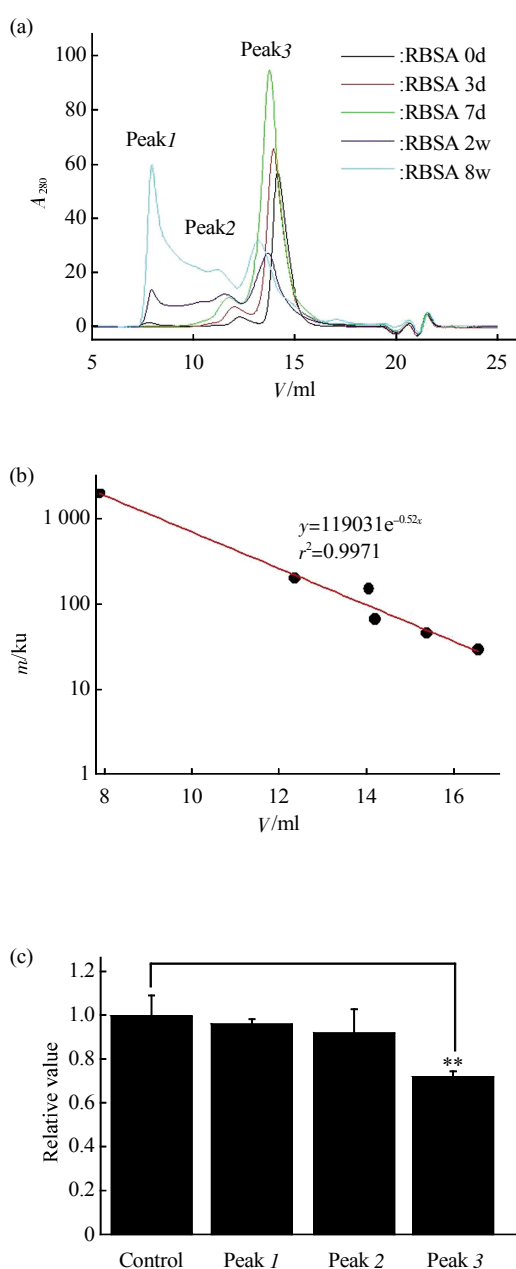


Fig. 6 Ribosylated monomer in severe cytotoxicity except for oligomer and polymer

(a) Size exclusion chromatography was used to separate and calculate particle sizes of ribosylated BSA at different time intervals as described in Figure 1a. Ribosylated BSA for 0d, 3d and 7d mainly showed one peak, while 2w and 8w showed three peaks. (b) The standard curve for molecular mass calculation of gel filtration calibration. Gel filtration calibration kit was used to calculate the standard curve. Y-axis represented molecular mass and X-axis represented elution volume. The molecular mass of ribosylated BSA can be determined from the calibration curve. (c) SH-SY5Y cells were cultured with the protein of three peaks separated from 8-week-ribosylated BSA for 24 h and cell viability was measured by CCK-8 assay. The control value was set as 1.0. All values are expressed as mean ± SEM. ** $P < 0.01$.

Table 1 Calculated particle sizes according to size exclusion chromatography

Sample	V/ml	m/ku	d/nm
RBSA 0d	14.17	66.45	7.22
RBSA 3d	13.95	74.49	7.37
RBSA 7d	13.75	82.26	7.52
RBSA 2W peak 1	7.95	1 652.83	36.52
RBSA 2W peak 2	11.58	292.08	10.67
RBSA 2W peak 3	13.69	85.03	7.57
RBSA 8W peak 1	7.94	1 661.40	36.67
RBSA 8W peak 2	11.17	312.84	11.77
RBSA 8W peak 3	13.23	107.85	7.99

AGEs exert the intracellular effect through interaction with its receptor on the cell membrane, receptor for advanced glycation end products (RAGE)^[34]. To investigate the involvement of RAGE and MAP kinases in the cellular effect of ribosylated BSA, we used the antibody against RAGE to block the interaction of AGEs (here is glycated BSA with ribose) with its receptor. As shown in Figures 7e and 7f, blockage of RAGE rescued cells in the presence of the cytotoxicity of ribosylated BSA, demonstrated by CCK-8 (Figure 7e) and released LDH activity assays (Figure 7f). The phosphorylated levels of MAP kinases were also detected (Figure 7g). Both p-Erk/Erk (Figure 7h) and p-p38/p38 (Figure 7i) in the cells were significantly down-regulated ($P < 0.05$, $n = 3$) after the AGEs-RAGE blockage, compared with 7-day-ribosylated BSA treatment group alone. All these data support that ribosylated BSA monomer induces cell death through activation of MAPK pathway.

3 Discussions

Glycation, a non-enzymic catalytic modification, is a severe risk factor for diabetic complications^[35] and neurodegenerative diseases^[36], by induction of protein aggregation, dysfunction and cell death^[37]. In this work, ribose, instead of glucose, was employed to study the mechanisms of glycation protein causing cell death due to ribose role in type 2 diabetes^[18]. Ribosylation of BSA was observed to form globular-like aggregations proceeding from monomer to oligomer and to polymer in a time dependent manner. The acquirement of cytotoxicity for glycated BSA is also dependent upon the time of ribosylation. The cytotoxicity from the highest to lowest of the BSA incubated with ribose was 7d > 2w > 3d > 8w. The 7-day-glycated protein acted

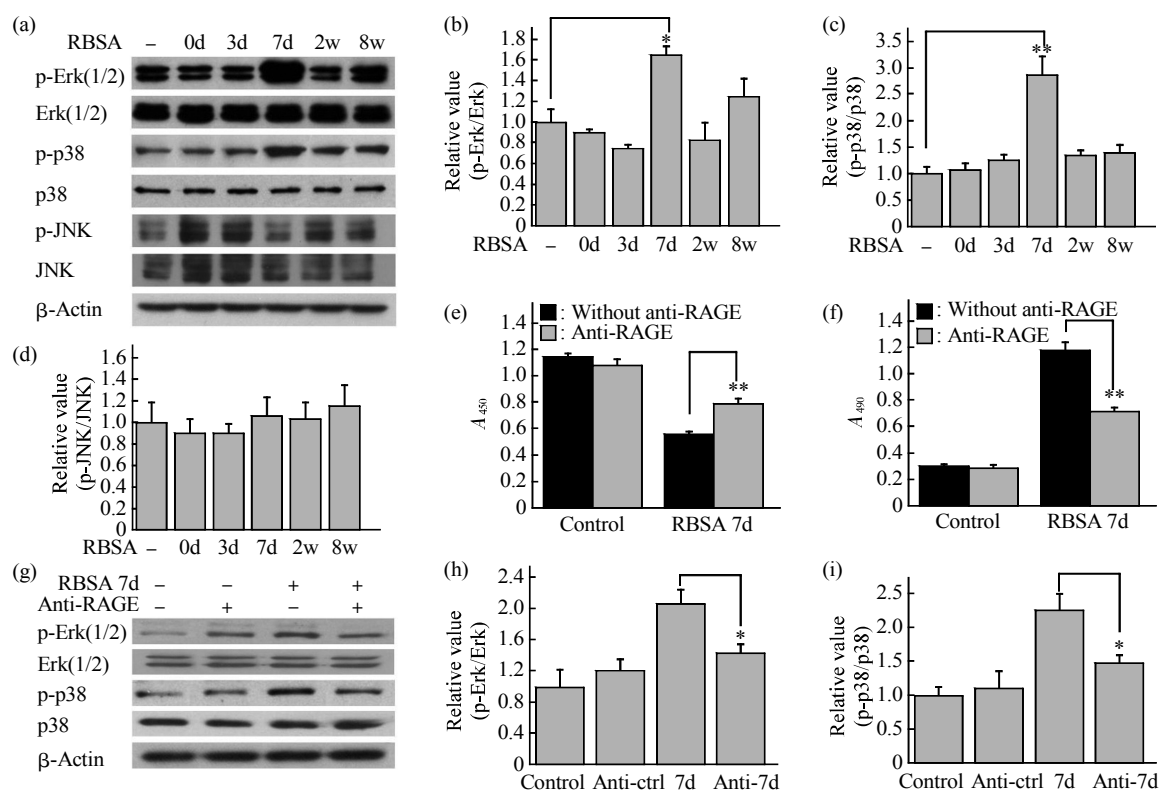


Fig. 7 Ribosylated BSA giving rise to cell death through MAPK pathway

(a) Western blotting of MAP kinases. Conditions for the cells treatment were the same as described in Figure 1b. Cell lysate extracts were separated by 12% SDS-PAGE and levels of MAP kinases were determined using monoclonal antibodies directed as activated or total kinases as follows: phospho-Erk/ total Erk, phospho-p38/ total p38, and phospho-JNK/ total JNK. β -Actin was used as a loading control. (b~d) Quantitative analyses of the data in Figure 7a. The control values were set as 1.0. All values are expressed as mean \pm SEM. * $P < 0.05$, ** $P < 0.01$. (e) RAGE antibody was pre-incubated for 2 h before 7-day-ribosylated BSA was added in SH-SY5Y for 24 h. Cells without ribosylated BSA were used as control. Cell viability was measured by CCK-8. All values are expressed as mean \pm SEM. ** $P < 0.01$. (f) The activity of LDH released from cells was detected under the same conditions as described in Figure 7e. All values are expressed as mean \pm SEM. ** $P < 0.01$. (g) Extracts of SH-SY5Y cell lysate (cells treatment as described in Figure 7e) were separated by 12% SDS-PAGE, and phosphorylation levels of MAP kinases were detected by using anti-p-Erk, anti-Erk, anti-p-p38 and anti-p38, respectively. β -Actin was used as a loading control. (h~i) Statistical results were shown. The control values were set as 1.0. All values are expressed as mean \pm SEM. * $P < 0.05$.

on RAGE, leading to cell apoptosis through activation of MAPK pathways.

Protein aggregation is a common feature in aging and neurodegenerative diseases^[38], including diabetes, Alzheimer disease and Parkinson disease^[39-40]. In AD, abnormal modification (such as phosphorylation and glycation) of tau protein is the main cause of tau aggregation^[41]. Others including gene mutation, the disruption of protein quality control system (chaperones and ubiquitin-proteasome system) and many environmental factors (such as oxidative stress and metal ions)^[42-43] can also induce protein aggregation. Recent reports have shown that immature protein aggregates are most toxic not the mature

protein aggregates^[44]. Oligomers, rather than polymers, of protein aggregates are thought to be cytotoxic^[19, 45], which is a milestone in the study of protein misfolding and aggregation. For example, soluble oligomer of A β rather than mature insoluble amyloid fibrils is regarded as the toxic aggregates causing loss of neurons in the progression of AD. Accumulating evidence indicated that a complex dynamic equilibrium exists between soluble states of monomer or oligomer and various insoluble states of higher order aggregation in protein aggregation process^[46]. However, in our ribosylation system, it is indicated that modified BSA monomer is more toxic than its oligomer and polymer. As we know, this is the first time that showed protein

glycated monomer was highly cytotoxic.

Glycation produces AGEs containing reactive carbonyl compounds such as carboxymethyl-lysine^[47] and pentosidine^[48], which are harmful to cellular metabolism and cause cell death^[49]. Glycated protein resulted from glycation also affects cell viability. LDH activity and caspase3 activity assay showed that the purified ribosylated BSA plays a critical role in cytotoxicity and 7-day-ribosylated BSA is most severely cytotoxic under our experimental conditions (Figure 1). TUNEL assay further indicated that the strands of the genomic DNA are structurally compromised in the presence of 7-day-ribosylated protein, leading to a compromised DNA structure damage, decreased cell viability and cell apoptosis.

The monomer, oligomer and polymer of ribosylated BSA all exist in AGEs (Figure 6a and Table 1). However, 7-day-ribosylated protein had much stronger cytotoxicity than the protein treated with ribose either less or longer than 7 days. A lower toxicity of 3-day-ribosylated BSA produced much less glycated monomer recognized by gel-filtration. It showed a less yield of glycated monomer, suggesting that a relatively low toxicity of 3-day-incubated protein is resulted from a low level of ribosylated product. At the same time, the size of 7-day-treated BSA was larger than 3-day-treated one, and this may resulted from different levels of glycation. On the other hand, 2-week- and 8-week-ribosylated BSA distinctly had low cytotoxicity though they produced abundant of AGEs. Seven-day-ribosylated BSA were mostly monomers, while 8-week-ribosylated BSA were polymers or even high molecular mass polymers. This suggests that the cytotoxicity of the ribosylated BSA is not only correlated with the level of glycation, but also depends on their particle sizes under the experimental conditions.

It is ribosylated monomer, neither oligomer nor polymer that has the severe cytotoxicity. This viewpoint is based on the following observations. First, AFM showed that the size (height) of the 7-day-glycated particles is (6.82±0.21) nm (Figure 4b). Second, transmission electron microscopy exhibited that the diameter of ribosylated protein on day 7 is (7.13±0.12) nm (Figure 5g), similar to the monomer size of BSA. Third, we measured the size of protein with gel-filtration and the fraction on day 7 incubation showed at peak 3 with the diameter ~7.52 nm for the glycated BSA (Table 2). Finally, we purified the

monomer (fraction of peak 3) and performed it with CCK-8 assay of cell viability. In the light of the Stokes diameter of BSA monomer (6.96 nm)^[50], it is the glycated monomer that is more toxic than the oligomer and polymer.

Table 2 Measurements of diameters of ribosylated BSA with different methods

	<i>d</i> (Ribosylated BSA)/nm	<i>d</i> (Native BSA)/nm
AFM	6.82±0.21	3.21±1.25
TEM	7.13±0.12	4.41±0.06
Gel-filtration	~7.52	~7.22
Stokes diameter ¹⁾	-	6.96

Ribosylated BSA referred to 7-day-ribosylated BSA. ¹⁾See reference Axelsson I.J Chromatogr, 1978^[50].

Ribosylated BSA monomer triggered apoptosis by the activation of MAPK pathway in the cells through the interaction of AGEs and RAGE on the cell membrane. Again, ribosylation induced BSA aggregation from monomer to oligomer and to polymer along the incubation time. On day 7 during the treatment, the glycated protein mainly existed in monomer with an obvious characteristic in AGEs and showed the highest cytotoxicity. Using the size exclusion chromatography, the components in peak 3 were mostly monomers, exhibiting that the ribosylated monomer was most strongly toxic. By using western blotting, we found that ribosylated BSA induced the activation of MAPK pathway (Figures 7a ~d). After blocking the AGEs-RAGE binding, the cytotoxicity of 7-day-ribosylated BSA markedly decreased (Figures 7e and 7f). This is to say, ribosylated BSA monomer acts on RAGE and plays its role in cytotoxicity. However, ribosylated BSA polymers (2w and 8w), which should produce more AGEs than ribosylated BSA (7d), showed no significant cytotoxicity. This suggests that ribosylated monomer may share the same signal pathway with AGEs leading to neuronal death. Therefore, ribosylated BSA acquires its high cytotoxicity that depends upon the characteristic of AGEs and the specific size of monomer.

In conclusion, by using glycation with ribose, we have observed BSA ribosylation and aggregation process, and found that ribosylated BSA aggregates into globular-like deposits proceeding in monomer, oligomer and polymer. However, ribosylated BSA monomer, neither oligomers nor polymers, showed

severe cytotoxicity that induces neuronal apoptosis through activation of MAPK pathways.

Acknowledgements We thank Prof. Sarah Perrett who works in the Institute of Biophysics (IBP), Chinese Academy of Sciences (CAS) for the gel filtration reagents. We also thank Ms. JIA Yan-Xia and Mr. JI Gang (IBP, CAS) for processing the AFM and TEM imaging and Mr. JIA Jun-Ying (IBP, CAS) for flow cytometry technique support. Dr. Robert Hatch (Queensland Brain Institute, The University of Queensland, Brisbane, Australia) edited the language of this paper.

References

- [1] Ahmed N, Thornalley P J. Advanced glycation endproducts: what is their relevance to diabetic complications? *Diabetes Obes Metab*, 2007, **9**(3): 233–245
- [2] Vasdev S, Gill V, Singal P. Role of advanced glycation end products in hypertension and atherosclerosis: therapeutic implications. *Cell Biochem Biophys*, 2007, **49**(1): 48–63
- [3] Head K A. Peripheral neuropathy: pathogenic mechanisms and alternative therapies. *Alternative Medicine Review: a Journal of Clinical Therapeutic*, 2006, **11**(4): 294–329
- [4] Karachalias N, Babaei-Jadidi R, Ahmed N, *et al.* Accumulation of fructosyl-lysine and advanced glycation end products in the kidney, retina and peripheral nerve of streptozotocin-induced diabetic rats. *Biochemical Society Transactions*, 2003, **31**(Pt 6): 1423–1425
- [5] Varkonyi T, Kempler P. Diabetic neuropathy: new strategies for treatment. *Diabetes Obes Metab*, 2008, **10**(2): 99–108
- [6] Thornalley P J. Glycation in diabetic neuropathy: characteristics, consequences, causes, and therapeutic options. *International Review of Neurobiology*, 2002, **50**: 37–57
- [7] Li L, Holscher C. Common pathological processes in Alzheimer disease and type 2 diabetes: a review. *Brain Research Reviews*, 2007, **56**(2): 384–402
- [8] Cameron N E, Gibson T M, Nangle M R, *et al.* Inhibitors of advanced glycation end product formation and neurovascular dysfunction in experimental diabetes. *Annals of the New York Academy of Sciences*, 2005, **1043**: 784–792
- [9] Giusti C, Gargiulo P. Advances in biochemical mechanisms of diabetic retinopathy. *European Review for Medical and Pharmacological Sciences*, 2007, **11**(3): 155–163
- [10] Su T, Xin L, He Y G, *et al.* The Abnormally high level of uric D-ribose for type-2 diabetics. *Prog Biochem Biophys*, 2013, **40**(9): 816–825
- [11] Su T, He R Q. D-ribose, an overlooked player in type 2 diabetes mellitus? *Sci China Life Sci*, 2014, **57**(3): 361–361
- [12] Wei Y, Chen L, Chen J, *et al.* Rapid glycation with D-ribose induces globular amyloid-like aggregations of BSA with high cytotoxicity to SH-SY5Y cells. *BMC Cell Biology*, 2009, **10**: 10
- [13] Chen L, Wei Y, Wang X, *et al.* D-Ribosylated Tau forms globular aggregates with high cytotoxicity. *Cellular and Molecular Life Sciences: CMLS*, 2009, **66**(15): 2559–2571
- [14] Lu J, Li T, He R, *et al.* Visualizing the microtubule-associated protein tau in the nucleus. *Sci China Life Sci*, 2014, **57**(4): 422–431
- [15] Chen L, Wei Y, Wang X, *et al.* Ribosylation rapidly induces alpha-synuclein to form highly cytotoxic molten globules of advanced glycation end products. *PLoS One*, 2010, **5**(2): e9052
- [16] Kong F L, Cheng W, Chen J, *et al.* d-Ribose glycates beta (2) -microglobulin to form aggregates with high cytotoxicity through a ROS-mediated pathway. *Chemico-biological Interactions*, 2011, **194**(1): 69–78
- [17] Han C, Lu Y, Wei Y, *et al.* D-ribosylation induces cognitive impairment through RAGE-dependent astrocytic inflammation. *Cell Death Dis*, 2014, **5**: e1117
- [18] Su T, He R Q. An insight of D-ribose metabolic imbalance in type 2 diabetes mellitus. *Prog Biochem Biophys*, 2015, **42**(4): 390–392
- [19] Stefani M, Dobson C M. Protein aggregation and aggregate toxicity: new insights into protein folding, misfolding diseases and biological evolution. *J Mol Med (Berl)*, 2003, **81**(11): 678–699
- [20] Williams T L, Johnson B R, Urbanc B, *et al.* Abeta42 oligomers, but not fibrils, simultaneously bind to and cause damage to ganglioside-containing lipid membranes. *The Biochemical Journal*, 2011, **439**(1): 67–77
- [21] Jeong H R, An S S. Causative factors for formation of toxic islet amyloid polypeptide oligomer in type 2 diabetes mellitus. *Clinical Interventions in Aging*, 2015, **10**: 1873–1879
- [22] Lin C Y, Gurlo T, Kayed R, *et al.* Toxic human islet amyloid polypeptide (h-IAPP) oligomers are intracellular, and vaccination to induce anti-toxic oligomer antibodies does not prevent h-IAPP-induced beta-cell apoptosis in h-IAPP transgenic mice. *Diabetes*, 2007, **56**(5): 1324–1332
- [23] Coussons P J, Jacoby J, McKay A, *et al.* Glucose modification of human serum albumin: a structural study. *Free Radical Biology & Medicine*, 1997, **22**(7): 1217–1227
- [24] Li Y P, Bushnell A F, Lee C M, *et al.* Beta-amyloid induces apoptosis in human-derived neurotypic SH-SY5Y cells. *Brain Research*, 1996, **738**(2): 196–204
- [25] Lindenboim L, Haviv R, Stein R. Inhibition of drug-induced apoptosis by survival factors in PC12 cells. *Journal of Neurochemistry*, 1995, **64**(3): 1054–1063
- [26] Zhang T H, Liu J F, Zhang Y, *et al.* Ceramide induces apoptosis in human lung adenocarcinoma A549 cells through mitogen-activated protein kinases. *Acta Pharmacologica Sinica*, 2007, **28**(3): 439–445
- [27] Chen S, Hou Y, Cheng G, *et al.* Cerium oxide nanoparticles protect endothelial cells from apoptosis induced by oxidative stress. *Biological Trace Element Research*, 2013, **154**(1): 156–166
- [28] Liu Y, Zhang S P, Cai Y Q. Cytoprotective effects of selenium on cadmium-induced LLC-PK1 cells apoptosis by activating JNK pathway. *Toxicology in vitro: an International Journal Published in Association with BIBRA*, 2007, **21**(4): 677–684
- [29] Wang L M, Li Q Y, Zu Y G, *et al.* Anti-proliferative and

- pro-apoptotic effect of CPT13, a novel camptothecin analog, on human colon cancer HCT8 cell line. *Chemico-Biological Interactions*, 2008, **176**(2-3): 165-172
- [30] Sakono M, Zako T. Amyloid oligomers: formation and toxicity of Abeta oligomers. *The FEBS Journal*, 2010, **277**(6): 1348-1358
- [31] Liu X M, Metzger L E. Application of fluorescence spectroscopy for monitoring changes in nonfat dry milk during storage. *J Dairy Sci*, 2007, **90**(1): 24-37
- [32] Erickson H P. Size and shape of protein molecules at the nanometer level determined by sedimentation, gel filtration, and electron microscopy. *Biol Proced Online*, 2009, **11**(1): 32-51
- [33] Alikhani M, Maclellan C M, Raptis M, *et al.* Advanced glycation end products induce apoptosis in fibroblasts through activation of ROS, MAP kinases, and the FOXO1 transcription factor. *American Journal of Physiology Cell Physiology*, 2007, **292**(2): C850-856
- [34] Xie J, Mendez J D, Mendez-Valenzuela V, *et al.* Cellular signalling of the receptor for advanced glycation end products (RAGE). *Cellular Signalling*, 2013, **25**(11): 2185-2197
- [35] Chiarelli F, Catino M, Tumini S, *et al.* Advanced glycation end products in adolescents and young adults with diabetic angiopathy. *Pediatr Nephrol*, 2000, **14**(8-9): 841-846
- [36] Wu B, Wei Y, Wang Y, *et al.* Gavage of D-ribose induces abeta-like deposits, Tau hyperphosphorylation as well as memory loss and anxiety-like behavior in mice. *Oncotarget*, 2015, **6**(33): 34128-34142
- [37] Wei Y, Han C, Wang Y, *et al.* Ribosylation triggering Alzheimer's disease-like Tau hyperphosphorylation *via* activation of CaMKII. *Aging Cell*, 2015, **14**(5): 754-763
- [38] Lansbury P T, Lashuel H A. A century-old debate on protein aggregation and neurodegeneration enters the clinic. *Nature*, 2006, **443**(7113): 774-779
- [39] Bartlett P F, He R Q. Introduction to the thematic issue "From brain function to therapy". *Sci China Life Sci*, 2014, **57**(4): 363-365
- [40] Zhou H L, Mangelsdorf M, Liu J H, *et al.* RNA-binding proteins in neurological diseases. *Sci China Life Sci*, 2014, **57**(4): 432-444
- [41] Whittington R A, Virag L, Gratuze M, *et al.* Dexmedetomidine increases tau phosphorylation under normothermic conditions *in vivo* and *in vitro*. *Neurobiology of Aging*, 2015, **36**(8): 2414-2428
- [42] Chin-Chan M, Navarro-Yepes J, Quintanilla-Vega B. Environmental pollutants as risk factors for neurodegenerative disorders: Alzheimer and Parkinson diseases. *Frontiers in Cellular Neuroscience*, 2015, **9**: 124
- [43] Hiramatsu N, Chiang W C, Kurt T D, *et al.* Multiple mechanisms of unfolded protein response-induced cell death. *The American Journal of Pathology*, 2015, **185**(7): 1800-1808
- [44] Nordlund A, Oliveberg M. SOD1-associated ALS: a promising system for elucidating the origin of protein-misfolding disease. *HFSP Journal*, 2008, **2**(6): 354-364
- [45] Winner B, Jappelli R, Maji S K, *et al.* *In vivo* demonstration that alpha-synuclein oligomers are toxic. *Proc Natl Acad Sci USA*, 2011, **108**(10): 4194-4199
- [46] Wolff M, Unuchek D, Zhang B, *et al.* Amyloid beta oligomeric species present in the lag phase of amyloid formation. *PLoS One*, 2015, **10**(5): e0127865
- [47] Ansari N A, Moinuddin, Ali R. Glycated lysine residues: a marker for non-enzymatic protein glycation in age-related diseases. *Disease Markers*, 2011, **30**(6): 317-324
- [48] Dyer D G, Blackledge J A, Thorpe S R, *et al.* Formation of pentosidine during nonenzymatic browning of proteins by glucose-identification of glucose and other carbohydrates as possible precursors of pentosidine *in vivo*. *J Biol Chem*, 1991, **266**(18): 11654-11660
- [49] Hu S, He W, Liu Z, *et al.* The accumulation of the glycoxidation product N(epsilon)-carboxymethyllysine in cardiac tissues with age, diabetes mellitus and coronary heart disease. *The Tohoku Journal of Experimental Medicine*, 2013, **230**(1): 25-32
- [50] Axelsson I. Characterization of proteins and other macromolecules by Agarose-gel chromatography. *J Chromatogr*, 1978, **152**(1): 21-32

核糖糖基化 BSA 单体对 SH-SY5Y 细胞的毒性明显*

魏艳^{1)*} 王玉婧^{1,2)**} 吴蓓蓓^{1,2)} 张英豪¹⁾ 赫荣乔^{1)***}

(¹⁾中国科学院生物物理研究所, 脑与认知科学国家重点实验室, 北京 100101; (²⁾中国科学院大学, 北京 100049)

摘要 研究显示, 蛋白质异常修饰形成的寡聚体, 与其多聚体、淀粉样纤维相比, 具有更强的细胞毒性. 这一发现被认为是蛋白质错误折叠和聚集研究领域中的重要进展. 蛋白质的异常修饰如还原糖的非酶糖基化, 是糖尿病最基本的病理特征. 2型糖尿病患者尿液中的核糖浓度显著升高, 表明糖尿病不仅与葡萄糖代谢紊乱相关, 同时也与核糖代谢失调相关. 以牛血清白蛋白(BSA)为研究对象, 通过荧光分光光度计检测、原子力显微镜、透射电子显微镜观察以及分子排阻色谱分离, 观察到核糖糖基化能够诱导 BSA 聚集, 从单体、寡聚体逐渐形成多聚体. 通过 CCK-8 Kit、乳酸脱氢酶细胞活性检测、TUNEL 染色、caspase-3 活性检测以及流式细胞检测等方法, 发现核糖糖基化的 BSA 单体对 SH-SY5Y 细胞(人神经母细胞瘤细胞系)具有明显的毒性, 与此同时, 糖化寡聚体和多聚体没有表现出显著的毒性. 进一步研究发现, 核糖糖基化的 BSA 单体通过与 AGEs 的受体 RAGE 相互作用, 激活细胞内的 MAPK 通路, 从而导致细胞凋亡.

关键词 核糖, 糖基化, 核糖糖基化, 单体, 多聚体, 细胞毒性

学科分类号 Q25

DOI: 10.16476/j.pibb.2016.0054

* 国家重点基础研究发展计划(973)(2012CB911004), 国家自然科学基金(31270868, 31200601)和中国科学院对外合作重点项目(GJHZ201302)资助.

** 共同第一作者.

*** 通讯联系人.

Tel: 010-64889876, E-mail: herq@sun5.ibp.ac.cn

收稿日期: 2016-02-23, 接受日期: 2016-05-11